NAVIGATION-AIDED AUTOMOTIVE SAR IMAGING IN URBAN ENVIRONMENTS

M. Rizzi[1], D. Tagliaferri[1], S. Tebaldini[1], M. Nicoli[1], I. Russo[2], C. Mazzucco[2], A.V. Monti-Guarnieri[1], C.M. Prati[1], U. Spagnolini[1]

[1]Politecnico di Milano, Milan, Italy
[2]Huawei Technologies Italia S.r.l., Segrate, Italy

ABSTRACT

Automated driving requires a huge number of on-board sensors to provide advanced functionalities, from parking assistance to emergency braking and environment mapping for target recognition/classification. While low-cost automotive-legacy radars are mostly used for target detection due to their limited angular resolution, vehicular Synthetic Aperture Radar (SAR) is emerging as a promising imaging solution, provided that the motion is known with high accuracy. This paper assesses the benefits of a navigation-augmented SAR system exploiting multiple on-board sensors, e.g., Global Navigation Satellite System (GNSS), Inertial Measurement Units (IMUs), odometers and steering angle sensors. The results confirm the potential of the proposed multi-sensor-aided SAR system to obtain centimeter-level accurate images of the driving scenario.

Index Terms— Automotive SAR, Sensor Fusion, Environment Mapping, Autonomous Driving

1. INTRODUCTION

Current state of the art Advanced Driver Assistance Systems (ADAS) for autonomous driving rely on a wide set of heterogeneous sensors, such as cameras, ultra-sonic sensors, lidars and millimeter-wave radars (working in W-band), to perform a number of operations, from parking to line change assistance and environment mapping for target recognition and classification. In particular, the latter is recognized as the key enabler of fully automated driving systems [1]. The goal is to image the driving scenario of a vehicle, identifying any kind of static and non-static targets such as buildings, poles, pedestrians, other vehicles, etc. Today's on-board sensors are characterized either by a low angular/range resolution trade-off (mass-market, automotive-legacy radars [2]) or by the inability to work in adverse weather conditions (lidars, cameras). Synthetic Aperture Radar (SAR) techniques appear as a promising solution to overcome the previous limitations, allowing to enhance the angular resolution of automotive-legacy radars by exploiting the ego-vehicle motion, which must be estimated with high precision. Errors in motion estimation (especially along the ranging direction) result in SAR images to appear at different positions, rotated and stretched. Traditionally, the residual motion compensation in airborne SAR systems is performed offline from radar and navigation data or even from radar data only, leveraging on fixed targets [3] (autofocusing methods). However, the major challenge for automotive systems is to operate in real-time (or quasi-real-time), and with cost-effective sensor setups. The estimation of arbitrary vehicle ego-motions from scratch (especially in highly-dynamic scenarios) or the usage of high-performance and high-cost navigation systems is not practical. Early research works on automotive SAR [4, 5] underline the need of knowing the radar motion along the synthetic aperture with high precision, analyzing by simulations the effect of a non-straight motion and proposing simple accelerometer- and/or gyroscope-based compensations. In [6], an experimental side-looking SAR system, mounted on the vehicle's rooftop, is used to demonstrate the applicability of automotive SAR imaging at a resolution of 15 cm, using an high-precision (and expensive) Inertial Navigation System (INS), integrating high-precision Inertial Measurement Unit (IMU) (accelerometers and gyroscopes) and Global Navigation Satellite System (GNSS) data. The more the resolution, the higher the requested quality of navigation data, as shown in [7], where a 300 GHz SAR demonstrator (40 GHz bandwidth) provides a millimeter-level accurate scene reconstruction, observed along a perfectly straight path moving at low speed. This work aims at exploiting multiple, heterogeneous on-board sensors, purposely mounted on the ego-vehicle terminal such as GNSS, IMU, wheel-based velocity sensors and steering angle sensor, to support automotive SAR imaging over typical urban driving scenarios. The results show the possibility of centimeter-accurate imaging without additional autofocusing approaches over non-straight tracks with non-uniform velocities.

2. DATA ACQUISITION CAMPAIGN

The dedicated acquisition campaign provided the radar and navigation data used to demonstrate the potential of high-precision urban SAR imaging. We employed a fully sensorized Alfa Romeo Giulia "veloce", sketched in Fig. 1,

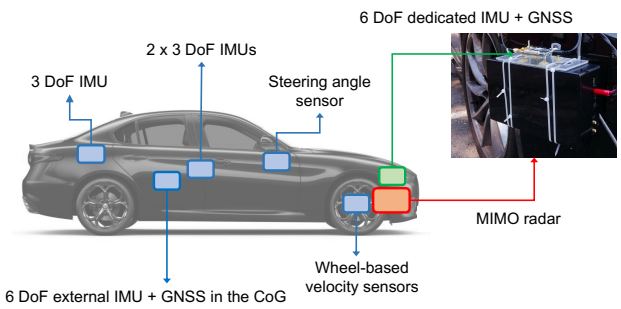

Fig. 1. Sensor set-up: blue boxes represent on-board sensors, green boxes the additional sensor installed for the campaign and the red box the ScanBrick® MIMO radar.

equipped with an external ScanBrick® W43 radar (proprietary platform by Aresys) rigidly mounted on the front bumper of the vehicle, about 0.5 m above ground, and pointed at 60 degrees with respect to the driving direction (frontal-side looking). The ScanBrick® is a short range (27 m maximum) Frequency Modulated Continuous Wave (FMCW) 3×4 MIMO radar operating in the 77-81 GHz band (3 GHz employed bandwidth) with a Pulse Repetition Frequency (PRF) of 990 Hz. The ScanBrick® is based on commercial automotive technology suitable for future marketability.

The car on-board sensor equipment consists of: *(i)* two co-located 3 Degrees of Freedom (DoF) IMUs, measuring lateral and longitudinal acceleration, along with heading rate; *(ii)* a 6 DoF IMU plus a GNSS module from Suchy Data Systems GmbH [8] in the vehicle Center of Gravity (CoG), measuring 3D acceleration and 3D angular velocity; *(iii)* an additional 3 DoF IMU in the rear part of the car; *(iv)* four wheel encoders measuring the odometric velocity of each wheel; *(v)* a steering angle sensor at the frontal wheels. In addition, a SAR-dedicated 6 DoF IMU+GNSS integrated sensor, from Inertial Sense [9], is rigidly mounted on top of the Scanbrick® radar (Fig. 1), aimed at providing a ground truth measurement of the radar 3D acceleration and 3D angular velocity. Finally, a 360 deg video camera has been placed on the vehicle rooftop to cross-check the acquired data.

3. DATA PROCESSING

In the following, we briefly describe the navigation and radar data processing applied to experimental data.

3.1. Navigation Data Processing

Navigation data from the on-board sensors are fused with an Unscented Kalman Filter (UKF) [10] to track the 2D radar position, the planar velocity and the orientation (heading) over time, which constitute the state to be tracked. We choose the Constant Turn Rate and Velocity (CTRV) model to describe the state evolution over time, that best represents the dynamics experienced in the experimental campaign, characterized by slowly varying speeds and heading rates. The measurements of on-board sensors (Section 2) compose the set of observations for the UKF. The IMU biases, which detrimentally affect navigation, are pre-calibrated from initial set-up (no motion) periods and subtracted from useful data.

3.2. Radar Data Processing

Radar data processing consists in a FMCW-specific step followed by SAR focusing. The first phase achieves the Range-Compressed (RC) data matrix $d_{RC}(t;\tau)$, function of the fast-time t and slow-time τ, collecting the sum of RC echoes from each target [11]; the second phase forms the radar image. Typical automotive trajectories, characterized by non-straight motions and non-uniform speeds, call for a Time Domain Back-Projection (TDBP)-based approach in the focusing phase. TDBP, in fact, yields an exact reconstruction of the observed space, given the knowledge of the radar motion along the synthetic aperture [11]. To diminish the computational complexity of standard TDBP, we take advantage of stripmap SAR processing, limiting the Field-of-View (FoV) by enforcing a spatial filter $W(\psi(\tau;x,y))$ on the angles of arrival ψ. The TDBP integral is therefore:

$$I(x,y) = \iint W(\psi(\tau;x,y)) \times \\ \times\ d_{RC}(t,\tau)\, s^{*}_{RC}(t;T_D(\tau;x,y))\ \mathrm{d}t\,\mathrm{d}\tau. \quad (1)$$

where $I(x,y)$ is the radar image and

$$T_D(\tau;x,y) = \frac{2}{c}\sqrt{(x-p_x(\tau))^2 + (y-p_y(\tau))^2} \quad (2)$$

is the two-way propagation delay between any given point of the radar trajectory $(p_x(\tau),\, p_y(\tau))$ (estimated by the UKF) and the 2D grid coordinates (x,y) ($c = 3 \times 10^8$ m/s). $s_{RC}(t;T_D(\tau;x,y))$ is the reference RC signal used by the FMCW system (* denotes the complex conjugate), equal to:

$$s_{RC}(t;T_D) = T_p\,\mathrm{sinc}\,[B(t-T_D)]\exp(j2\pi f_0 T_D) \quad (3)$$

where f_0 id the carrier frequency, B is the employed bandwidth and T_p is the chirp duration and $\mathrm{sinc}\,[x] = \sin(x)/x$. The range resolution, ruled by the system bandwidth $B = 3$ GHz, is 5 cm and the spatial filter $W(\psi(\tau;x,y))$ is here designed such that to achieve the same resolution in cross-range.

4. RESULTS

Radar and navigation data were collected on a closed road in front of the Dipartimento di Elettronica, Informazione e Bioingegneria (DEIB) of Politecnico di Milano. We report the results concerning two tracks of approximately 50 m (Test 1) and 100 m (Test 2) length, from East to West and vice versa,

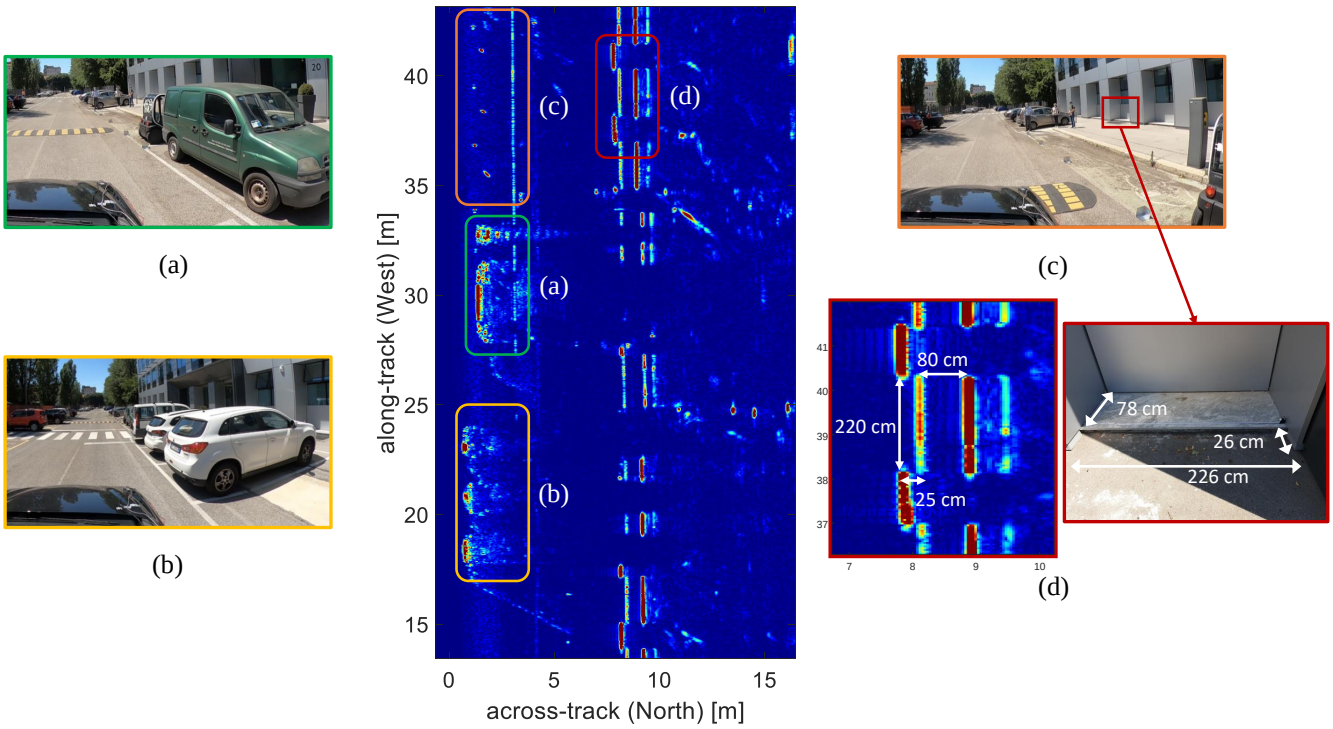

Fig. 2. Test 1: SAR image target identification (image not in scale).

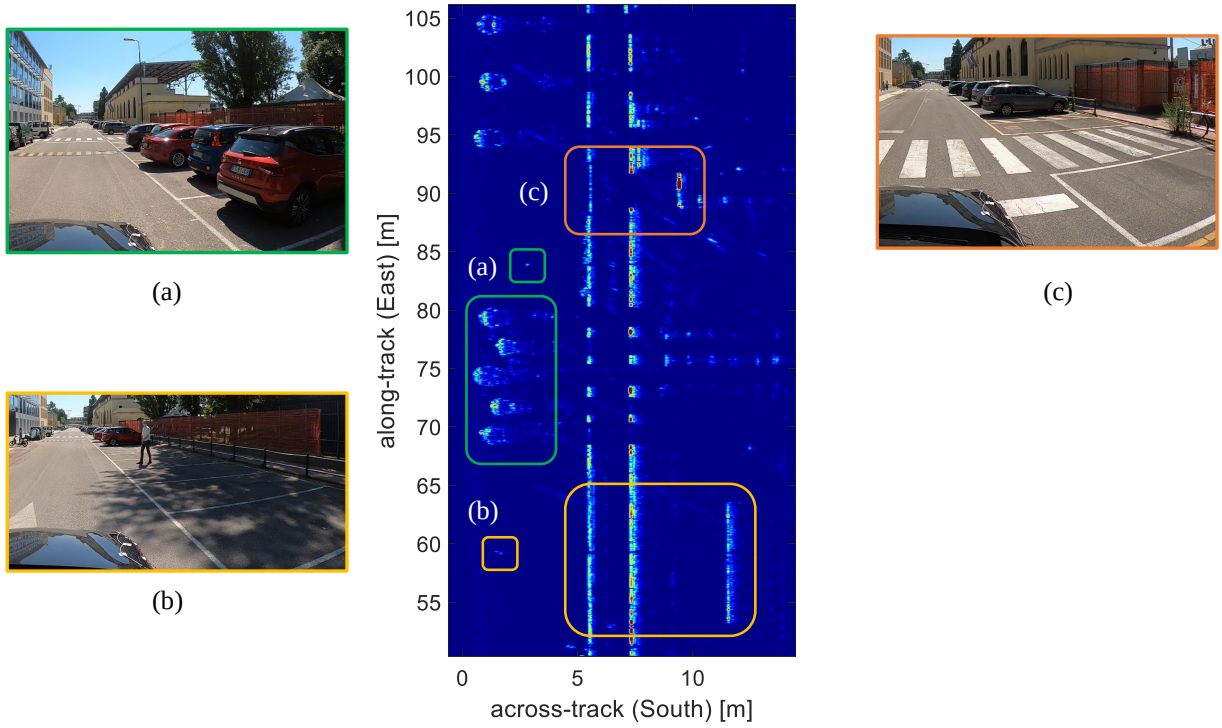

Fig. 3. Test 2: SAR image target identification (image not in scale).

where the vehicle deviates of about ± 1.5 m from a perfectly straight motion. In both tests, the vehicle's speed was limited to 20 km/h by the PRF of the radar to obtain unambiguous image formation, and, importantly, the images are obtained without autofocusing. The set of available targets comprise parked cars, the DEIB's facade, a sidewalk, various structures at the roadside, pedestrians and reflective corners placed along the observed scene. Snapshots form the video camera recordings help the target identification in the following SAR images.

The focused image of the observed scene during the first trajectory (Test 1) is reported in Fig. 2. In particular, it is immediate to distinguish the mini-van and the electric car (a), a series of parked vehicles side-by-side (b), and the set of corners in front of the side-walk (c). Remarkably, the geometry of structures such as the side-walk and the DEIB's facade are accurately reconstructed (within few centimeters), as shown in (d), thanks to the multi-sensor ad-hoc ego-vehicle navigation supporting SAR imaging.

Similar results are reported in Fig. 3 for Test 2. Parked cars of different size and the nearby lamppost are highlighted in (a). Of great importance, pedestrian targets are identifiable (b) and, additionally, constructions at the side of the road (fences and a storage room) are focused accurately (b), (c).

5. CONCLUSION

This study confirms the potential of navigation-aided automotive SAR for centimeter-level accuracy mapping of the environment, employing multiple heterogeneous sensors onboard the car and an off-the-shelf radar platform. The precise estimation of the radar motion provided by an ad-hoc sensor data fusion turns out to be a key enabler for correct image formation. Future works are expected to increment the maximum velocity for correct imaging and stress the need for real-time processing for autonomous driving applications.

6. ACKNOWLEDGMENT

The research has been carried out in the framework of the Huawei-Politecnico di Milano Joint Research Lab on automotive SAR. The Authors want to acknowledge Dr. Paolo Falcone from Aresys for the cooperation and support in the data acquisition campaign, as well as Prof. Sergio Savaresi for the availability of the Alfa Romeo car.

7. REFERENCES

[1] E. Marti, M. A. de Miguel, F. Garcia, and J. Perez, "A Review of Sensor Technologies for Perception in Automated Driving," *IEEE Intelligent Transportation Systems Magazine*, vol. 11, no. 4, pp. 94–108, 2019.

[2] J. Hasch, E. Topak, R. Schnabel, T. Zwick, R. Weigel, and C. Waldschmidt, "Millimeter-Wave Technology for Automotive Radar Sensors in the 77 GHz Frequency Band," *IEEE Transactions on Microwave Theory and Techniques*, vol. 60, no. 3, pp. 845–860, 2012.

[3] S. Tebaldini, F. Rocca, M. Mariotti d'Alessandro, and L. Ferro-Famil, "Phase Calibration of Airborne Tomographic SAR Data via Phase Center Double Localization," *IEEE Transactions on Geoscience and Remote Sensing*, vol. 54, no. 3, pp. 1775–1792, 2016.

[4] H. Wu and T. Zwick, "A novel motion compensation algorithm for automotive SAR : Simulations and experiments," in *German Microwave Conference Digest of Papers*, 2010, pp. 222–226.

[5] H. Wu, L. Zwirello, X. Li, L. Reichardt, and T. Zwick, "Motion compensation with one-axis gyroscope and two-axis accelerometer for automotive SAR," in *2011 German Microwave Conference*, 2011, pp. 1–4.

[6] R. Feger, A. Haderer, and A. Stelzer, "Experimental Verification of a 77-GHz Synthetic Aperture Radar System for Automotive Applications," in *2017 IEEE MTT-S International Conference on Microwaves for Intelligent Mobility (ICMIM)*, 2017, pp. 111–114.

[7] S. Stanko, S. Palm, R. Sommer, F. Klöppel, M. Caris, and N. Pohl, "Millimeter Resolution SAR Imaging of Infrastructure in the Lower THz region using MIRANDA-300," in *2016 European Radar Conference (EuRAD)*, 2016, pp. 358–361.

[8] Suchy Data Systems GmbH, *xProGPS nano Operating Manual*, 2019.

[9] Inertial Sense, *uIMU, uAHRS, uINS+RTK, uINS-Dual Calibrated Inertial Systems with Onboard GPS*, 2020.

[10] E. A. Wan and R. Van Der Merwe, "The Unscented Kalman Filter for Nonlinear Estimation," in *Proceedings of the IEEE 2000 Adaptive Systems for Signal Processing, Communications, and Control Symposium (Cat. No.00EX373)*, 2000, pp. 153–158.

[11] E. C. Zaugg and D. G. Long, "Generalized Frequency Scaling and Backprojection for LFM-CW SAR Processing," *IEEE Transactions on Geoscience and Remote Sensing*, vol. 53, no. 7, pp. 3600–3614, 2015.